Parameterized Updraft Mass Flux as a Predictor of Convective Intensity

John S. Kain
Cooperative Institute for Mesoscale Meteorological Studies
NOAA/National Severe Storms Laboratory

Michael E. Baldwin
Cooperative Institute for Mesoscale Meteorological Studies
NOAA/National Severe Storms Laboratory
NOAA/NWS Storm Prediction Center

Steven J. Weiss
NOAA/NWS Storm Prediction Center

Submitted as a Note to
Weather and Forecasting

March 2002

Abstract

Parameterized updraft mass flux, available as a unique predictive field from the Kain-Fritsch (KF) convective parameterization, is presented as a potentially valuable predictor of convective intensity. The version of the KF scheme currently being run in realtime in an experimental version of the Eta model is described in some detail. It is shown that updraft mass flux computed by this scheme is a function of the specific algorithm that it utilizes and it is quite sensitive to the thermodynamic characteristics of input soundings. These same characteristics appear to be related to the severity of convection, suggesting that updraft mass flux predicted by the KF scheme has value for predicting severe weather. This argument is supported by anecdotal evidence and a case study.

1. Introduction

Mesoscale models are used routinely to provide guidance in forecasting severe convection. For example, examination of output from the Environmental Modeling Center's (EMC's) Eta (Black 1994) and RUC-2 (Benjamin et al. 1998) models is a firmly entrenched part of the forecast preparation process at the National Weather Service's Storm Prediction Center (SPC), especially for the convective outlook product. In recent years, additional mesoscale models have become available and these are also consulted by SPC forecasters on occasion.

What sort of information do forecasters expect to glean from these various models? These models are often utilized for their predictions of synoptic-scale patterns, wind fields, etc. In addition, the models are capable of predicting mesoscale circulations and local thermodynamic structures that can provide valuable clues as to where convection might initiate and how it might evolve. As for the actual prediction of deep convection, however, forecasters receive the same information that has been provided for many years from coarser-resolution models. Specifically, they receive parameterized convective rainfall totals, typically accumulated over 3-6 h time periods.

It is unfortunate that operational models provide only this single measure of convective intensity because accumulated precipitation is a superficial and often ambiguous reflection of the vigor of convection. For example, the most significant severe thunderstorms typically occur in environments characterized by strong winds aloft (*e.g.*, Johns and Doswell 1992), which often results in fast moving storms that do not produce heavy amounts of rainfall at any one location. In addition, some severe thunderstorms produce minimal rainfall, such as low precipitation supercells (Bluestein and Parks 1983), or those associated with dry microbursts(Wakimoto 1985). Thus precipitation amounts do not necessarily correspond to the severity of convective storms.

Numerous other parameters that may reveal useful characteristics of predicted convection are computed internally in numerical weather prediction models, but these parameters are not provided as part of operational output. As forecasters become more educated users of numerical

models, they may benefit from more sophisticated, non-traditional output fields.

As part of our testing of experimental models at the National Severe Storms Laboratory (NSSL) and the SPC, we have been providing SPC forecasters with additional diagnostic terms that are routinely computed in the Kain-Fritsch (1993, hereafter KF) convective parameterization scheme (CPS). This CPS is used in place of the operational Betts-Miller-Janjic scheme (Janjic 1994) in our twice-daily runs of the Eta model at NSSL (hereafter "EtaKF"). The KF output field that has received the most favorable response from SPC forecasters is a normalized "updraft mass flux" (UMF*) predicted by the scheme. The magnitude of this field provides a measure of how much mass this CPS transports through cloud base as part of its internal procedure for stabilizing the local environment. As such, it provides a unique prediction of convective intensity, a measure that is not always well correlated with the precipitation rate or any other routinely available output field.

The purpose of this paper is two-fold. First, it is to provide a resource for forecasters who utilize models that contain the KF scheme and provide the UMF* output field. Second, it is to demonstrate the potential value of this unique output field and to encourage model developers to explore the use of non-traditional output fields to enhance the value of numerical models. We start by describing the procedure used by the KF scheme to remove instability in a convecting grid column and how UMF* fits into this procedure. Next, we explore the sensitivity of UMF* to various thermodynamic parameters in input soundings and discuss the relevance of this field to real physical processes. This is followed by presentation of a real-data example of the utility of UMF*, then concluding comments.

2. A description of the Kain-Fritsch convective parameterization

Most elements of the KF CPS have been described elsewhere (KF 1990, 1993), but a largely non-quantitative overview is presented here for completeness. The scheme is based on fixed-point observations of the changes that occur in atmospheric thermodynamic structure as a result

of deep moist convection (*i.e.*, Fritsch et al. 1976). Specifically, it is designed to simulate a vertical rearrangement of mass that allows the atmosphere to eliminate CAPE (Convective Available Potential Energy). This rearrangement occurs in the scheme through three vertical transport mechanisms: a moist convective updraft, a moist convective downdraft, and a dry branch of ascent or descent that is assumed to occur locally (*i.e.*, within a grid column) to compensate for the moist drafts. The third component is necessary for two reasons: 1.) A grid column in a model is divided into many vertical layers, and mass must be conserved in each layer during processing by the CPS; 2.) each grid column is completely closed off from its neighbors within the CPS, so mass compensation must be accomplished within the column.

The first task of the KF scheme is to evaluate potential *updraft- source layers (USLs)* to determine whether convection can be initiated and, if so, from what model layers unstable air would originate. The normalized (non-dimensional) UMF value that we provide as model output is the percentage of the mass in the USL that is actually processed by the CPS during each convective time period, *i.e.*,

$$UMF^* = \frac{UMF_{USL} \times \tau_c}{M_{USL}} \times 100, \qquad (1)$$

where UMF_{USL} is the updraft mass flux (kg s^{-1}) at the top of the USL, as determined by the parameterization, τ_c is the convective time period (s) and M_{USL} is the mass of air in the USL (kg). Typically, the maximum value of UMF* during the previous hour is provided at each grid point as hourly output from the model.

Potential USLs are evaluated as follows. Beginning at the surface, vertically adjacent model layers are mixed until the depth of the mixture is at least 50 hPa. This combination of adjacent model layers comprises the first potential USL. The mean thermodynamic characteristics of this mixture are computed, along with the temperature and height of this "parcel" at its lifting condensation level (LCL). The parcel is given a perturbation (as described in KF 1992) and the parcel buoyancy equation is used to determine whether it can reach its level of free convection (LFC). If it can reach the LFC and continue to rise beyond a specified minimum depth (typically 3-4 km), this USL is identified as the source for air that flows through cloud base. If not, the base of the

potential updraft source layer is moved up one model layer and the procedure is repeated. This process continues until either the first suitable source layer is found, or the sequential search has moved up above the lowest 300 hPa of the atmosphere, where the search is terminated. Since only one source layer is allowed to contribute in a given convective cycl $\tau_c \approx 30 min$ s() the parameterized updraft derives most of its mass from the lowest layer that is approximately 50 hPa deep and satisfies the above criteria. It is important to note that, since each grid column is considered independently in this procedure, the total amount of mass withdrawn from a source layer is limited to the amount of mass in that layer initially.

Once an USL has been identified, stabilization of a grid column is accomplished by the three vertical transport mechanisms. Each of the mechanisms plays an important role, as described below.

*a. Moist convective updraft*s

Convective updrafts in the KF scheme are represented using an enhanced formulation of a steady-state entraining plume, the details of which can be found in KF (1990). The plume model is based on Lagrangian parcel theory, which can be used to estimate updraft thermodynamic characteristics at each model level. Cloud top is established as the level (above the LFC) where vertically integrated lifted-parcel buoyancy goes to zero. Most of the condensate produced in the updraft is converted to precipitation (although some detrains into the environment) and a portion of this precipitation is used to drive an evaporatively cooled downdraft. The remaining precipitation arrives at the surface, giving the parameterized precipitation rate.

Updraft mass accumulates and modifies the environment only where detrainment is determined to occur. In many environments, almost all of the detrainment occurs within 100-200 hPa of cloud top, so significant direct modification of the environment by the parameterized updraft often occurs primarily near cloud top. Over most of the cloud layer, the parameterized updraft warms and dries the environment *indirectly.* Specifically, since the mass conservation imposed by

the scheme requires the air surrounding the updraft to subside, parameterized warming and drying in the cloud layer is usually dominated by vertical advection of temperature and water vapor in the clear-air environment.

b. Moist convective downdrafts

Moist downdrafts are also represented using an entraining plume model. In the version of the KF scheme used in the Eta model, a parameterized downdraft begins with zero mass flux about 150 hPa above the top of the USL and it entrains mass as a linear function of pressure-depth as it approaches the top of this layer. Thus, when it reaches the top of the USL, its θ_e value is equal to a mass-weighted mean of the environmental θ_e in the model layers between the top of the USL and 150 hPa above. This choice of downdraft source layer is qualitatively consistent with observations of low-level precipitation-driven downdrafts (Knupp and Cotton 1985; Knupp 1989). As the downdraft enters the USL, entrainment stops and detrainment begins. The detrainment layer extends downward to the point where parcels lose negative buoyancy or the surface is reached, and detrainment is distributed evenly over this layer. The relatively low θ_e air typically found in the downdraft entrainment layer replaces some of the unstable air that is extracted from the USL and this exchange is often the dominant mechanism of stabilization in the parameterization.

Efficient stabilization of the environment is favored when θ_e in the downdraft is much lower than θ_e in the updraft source layer, *i.e.*, a steep θ_e lapse rate exists. But, of course, this also depends also on how *much* downdraft mass is available for detrainment. In the version of the KF scheme currently being used in the Eta model, the *downdraft* mass flux (DMF) at the top of the detrainment layer (also the top of the USL) is specified as a fraction of the UMF according to

$$\frac{DMF_{USL}}{UMF_{USL}} = 2 \times (1 - \overline{RH}) \qquad (2)$$

where $\overline{RH}$ is the mean (fractional) relative humidity in the downdraft *entrainment* layer. So, for a given updraft, more downdraft mass is generated when the air just above the USL is dry. Conversely, downdraft mass flux decreases as air in this layer approaches saturation. This specific

formula is loosely based on modeling studies (*e.g.*, Ferrier et al. 1996) and sensitivity tests with the KF scheme. Factors such as stability profiles and vertical wind shear likely play some role in determining downdraft mass flux as well, but these effects are not included explicitly in the current formulation.

A third important factor is the depth of the detrainment layer. Recall that entrainment stops and detrainment begins at the top of the USL. The detraining mass is distributed evenly between the top of the USL and either 1) the layer where the downdraft loses its negative buoyancy, or 2) the ground. When the USL is in contact with the ground, downdraft mass detrainment is confined to the USL, which is the most efficient arrangement for lowering of θ_e in the USL. When the USL is elevated, however, the downdraft can penetrate below the base of the USL, spreading the (same amount of) detraining mass over a deeper layer. When this happens, less than 100% of the downdraft mass detrains within the USL and stabilization of the USL is less efficient. When this is the case, higher values of UMF* (and more specifically, DMF) are required to achieve the same lowering of θ_e in the USL. In general, with all other factors being equal, the KF scheme tends to produce higher UMF* values for elevated convection.

The amount of precipitation that is necessary to drive the downdraft through evaporative cooling effects is determined by the above mass-flux constraints and a specified relative humidity profile in the downdraft. In the version of the KF scheme currently being used in the Eta model, the downdraft is assumed to remain nearly saturated above the top of the USL, and then dry out at a rate of 20% relative humidity per km below this level. The drying rate is loosely based on Srivastiva (1985). In extreme cases (favored by a combination of a significantly elevated USL, dry air in the downdraft entrainment layer, high lapse rates below the USL) the DMF given by (2), coupled with the specified relative humidity profile, would evaporate more condensate than the updraft can provide. In these cases, the DMF value is reduced to the point where all of the condensate is just evaporated, so that the scheme generates no convective precipitation but still activates other convective tendencies.

c. Local compensating vertical motions

Once updraft and downdraft mass fluxes (of opposite sign) are determined, local compensating vertical motions are imposed so that the net vertical mass flux at any level in the column is zero. For a full-tropospheric cloud, this typically means that compensating subsidence produces heating and drying throughout most of the cloud layer. Subsidence rates may be weaker in the layer where DMF is non-zero (or compensating *upward* motion may even occur if -DMF>UMF), but typically the compensating motion is downward throughout the column. While this almost always induces warming and drying tendencies at each level, it also represents a vertical advection of θ_e, so it can augment downdraft effects by transporting lower θ_e air into the USL if θ_e is decreasing with height just above the USL (typically the case).

d. Method and implications of satisfying the KF closure

These representations of updraft, downdraft, and compensating environmental vertical motions allow the KF scheme to generally characterize the convective fluxes that would be likely to develop in a given unstable environment and they provide us with a first guess at the magnitude of the fluxes. The *relative* magnitudes of the different branches of the circulation are not allowed to change from this point, but the strength of the entire circulation typically requires an adjustment in order to remove CAPE in the column.

A convective time period is estimated (KF 1993) and the impact of the first-guess mass fluxes acting over this time period is computed. The CAPE value for the modified USL and cloud environment is then determined. If the modified CAPE is less than 10% of the original value (*i.e.*, at least 90% of the CAPE has been eliminated), the closure is satisfied and convective feedback magnitudes are set. Typically, the CAPE closure is not satisfied by the first guess values, so all mass fluxes are increased incrementally until the 10% criterion is satisfied. The CAPE reduction is accomplished by the combined effects of lowering θ_e in the USL and warming the environment

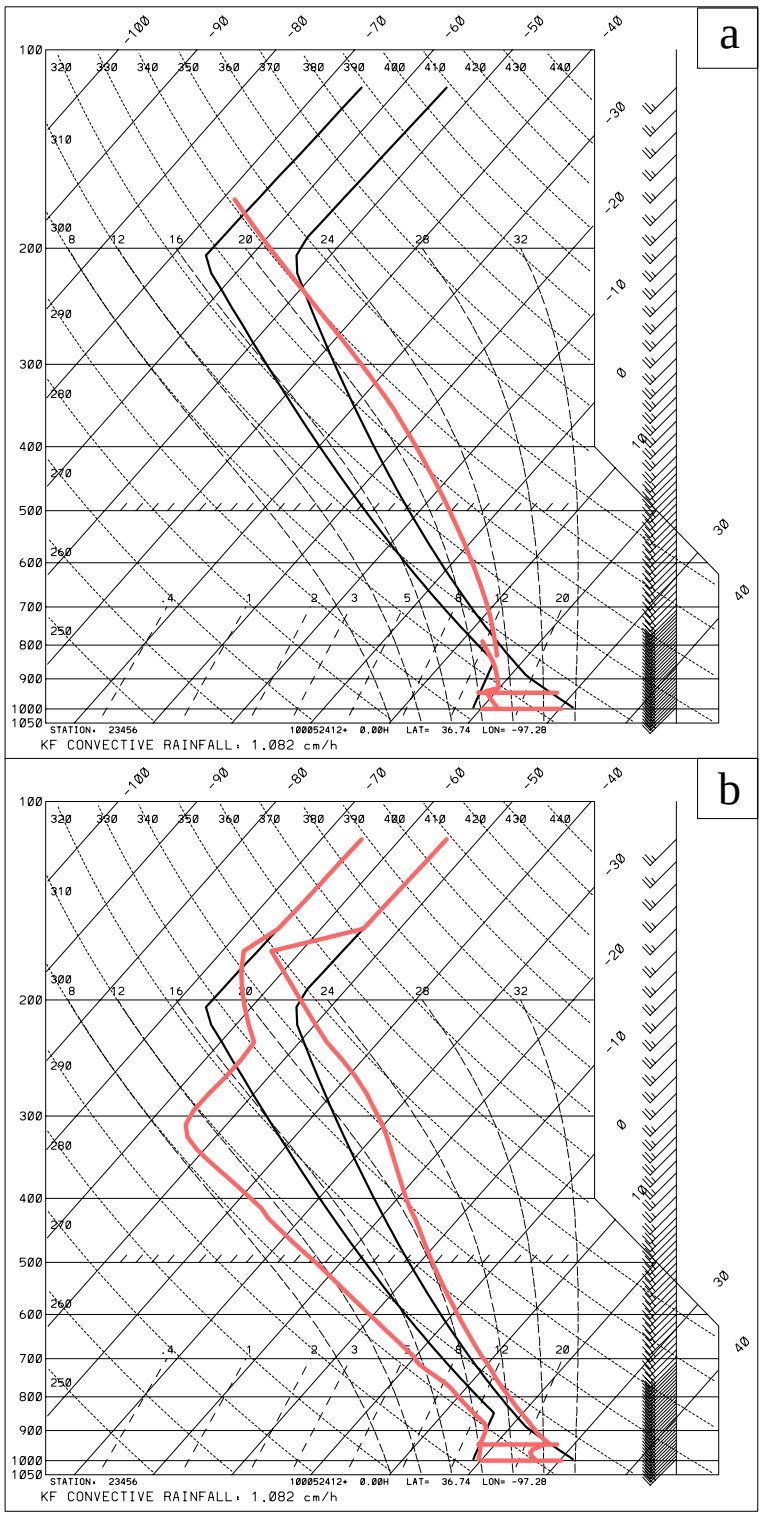

Fig. 1. An idealized sounding (thick dark curves) with a) the updraft and downdraft traces and b) the modified sounding resulting from mass rearrangements, both predicted by the KF scheme (thick lighter curves). The thick lighter horizontal lines near the surface denote the top and bottom of the updraft source layer (USL).

aloft

In order to demonstrate how the KF scheme operates and the sensitivity of computed UMF* to variations in sounding structure, we utilize an analytical sounding generator derived from Weisman and Klemp (1982). Fig. 1a shows a sample thermodynamic profile from this routine, along with the updraft and downdraft paths predicted by the scheme for this environment. Note that the updraft path deviates from a moist adiabat as a result of entrainment. The downdraft approaches the USL (denoted by thick parallel horizontal lines) with the mean wet-bulb temperature of its source layer (approximately 775-925 hPa). At this point it changes temperature abruptly because cooling due to melting precipitation is applied. Below this point (*i.e.*, in the detrainment layer) its θ_e value does not change, but its lapse rate increases because it is assumed to become sub-saturated. Modification of this environment by

the scheme is indicated in Fig. 1b. Note the strong cooling from downdraft detrainment in the USL (and from updraft detrainment above about 230 hPa) and the warming and drying through most of the cloud layer due to subsidence in the clear air.

3. UMF* as a diagnostic quantity

With the sounding generator routine, thermodynamic profiles can be systematically modified to evaluate the sensitivity of UMF* to vertical sounding structure. For comparison, we also plot the rainfall rate as a function of these different structures. For each of the soundings shown below, the USL is the lowest 50 hPa layer.

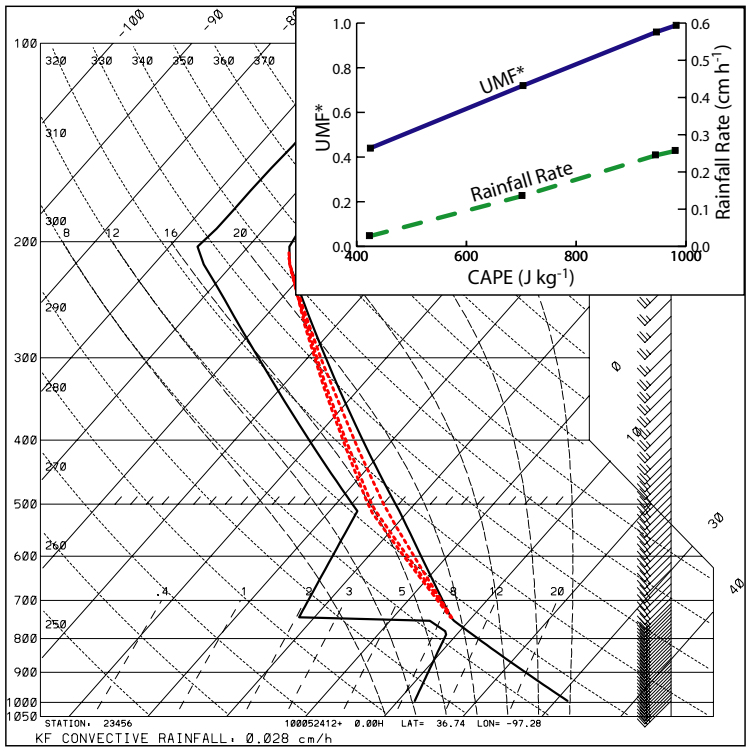

Fig. 2. Idealized sounding (solid curves) modified to evaluate the impact of increasing lapse rates in the 750-500 mb layer. Dashed lines show modified temperature profiles with higher lapse rates and CAPE values. Inset shows UMF* and rainfall rate predicted by the KF scheme as a function of the different (undilute parcel) CAPE values corresponding to the different temperature profiles.

a. Sensitivity to CAPE

UMF* can be quite sensitive to CAPE, but it also depends on the vertical distribution of CAPE. For example, Fig. 2 shows a series of soundings in which CAPE was modified by increasing the lapse rate between 750 and 500 hPa. It is important to recognize that in this series of modifications, θ_e values remain constant in both the USL (between 1000 and 950 hPa) and the downdraft source layer (between 950 and 800 hPa). As the inset plot in Fig. 2 indicates, CAPE increases from about 450 to 975 J kg^{-1} as the lapse rate is varied over the range shown on the Skew-T diagram. UMF* is

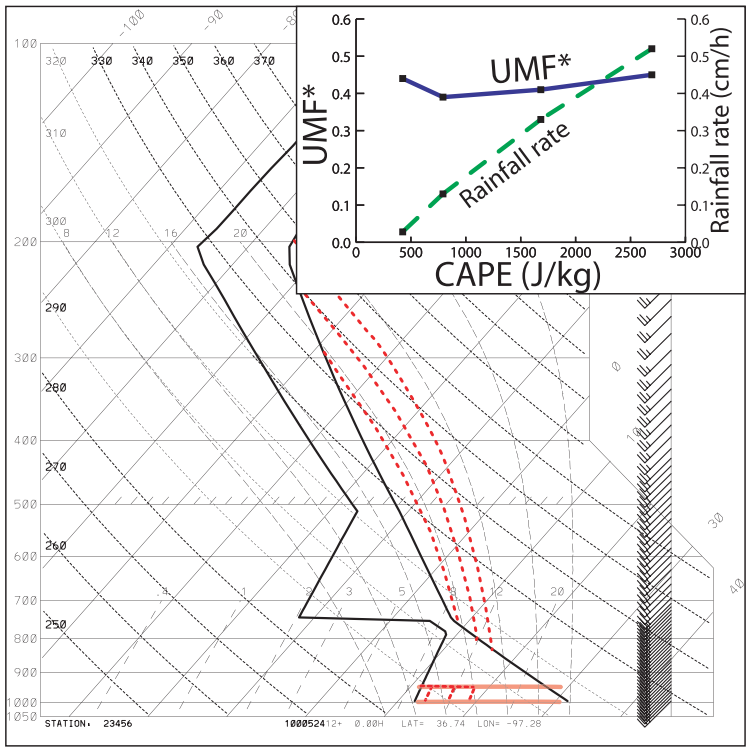

Fig. 3. Idealized sounding modified to evaluate the impact of moistening in the USL (top and bottom denoted by light thick horizontal lines near the surface). Thick dashed lines between 1000 and 950 mb indicate USL dewpoint profiles in different modified soundings while thick dashed lines aloft denote the undilute parcel trace corresponding to the modified USL dewpoints. Note that the input sounding is not modified above the top of the USL. Inset shows UMF* and rainfall rate computed by the KF scheme as a function of the different CAPE

shown to be quite sensitive to these modest changes in CAPE, increasing from about 0.44 for the lowest CAPE value to 1.0 for the highest. The parameterized rainfall rate increases as a similar monotonic function of CAPE, from about 0.05 cm h^{-1} to 0.27 cm h^{-1}.

UMF* responds very differently when CAPE is enhanced by increasing moisture (and θ_e) in the USL, while keeping θ_e constant in the downdraft source layer. For example, the inset in Fig. 3 shows that UMF* changes very little as CAPE values go from about 450 to 2700 J kg^{-1}. In contrast, the rainfall rate again increases monotonically as CAPE increases.

Although CAPE can be manifested in many ways, diagnostic tests reveal that UMF* values are more sensitive to the vertical distribution of CAPE than to its absolute magnitude. In particular, UMF* responds strongly when environmental lapse rates steepen in the lower to middle troposphere because more mass flux is required to produce the same amount of heating. Consider the scheme's compensating subsidence term, given by

$$\frac{\partial T}{\partial t} = -w(\Gamma_d - \gamma), \tag{3}$$

where T is temperature (K), t is time (s), w is the compensating subsidence (m s^{-1}), Γ_d is the dry-adiabatic lapse rate (K s^{-1}), and γ is the environmental lapse rate (K s^{-1}). Since w is directly proportional to the mass flux at every level, when γ approaches Γ_d, the updraft mass flux must

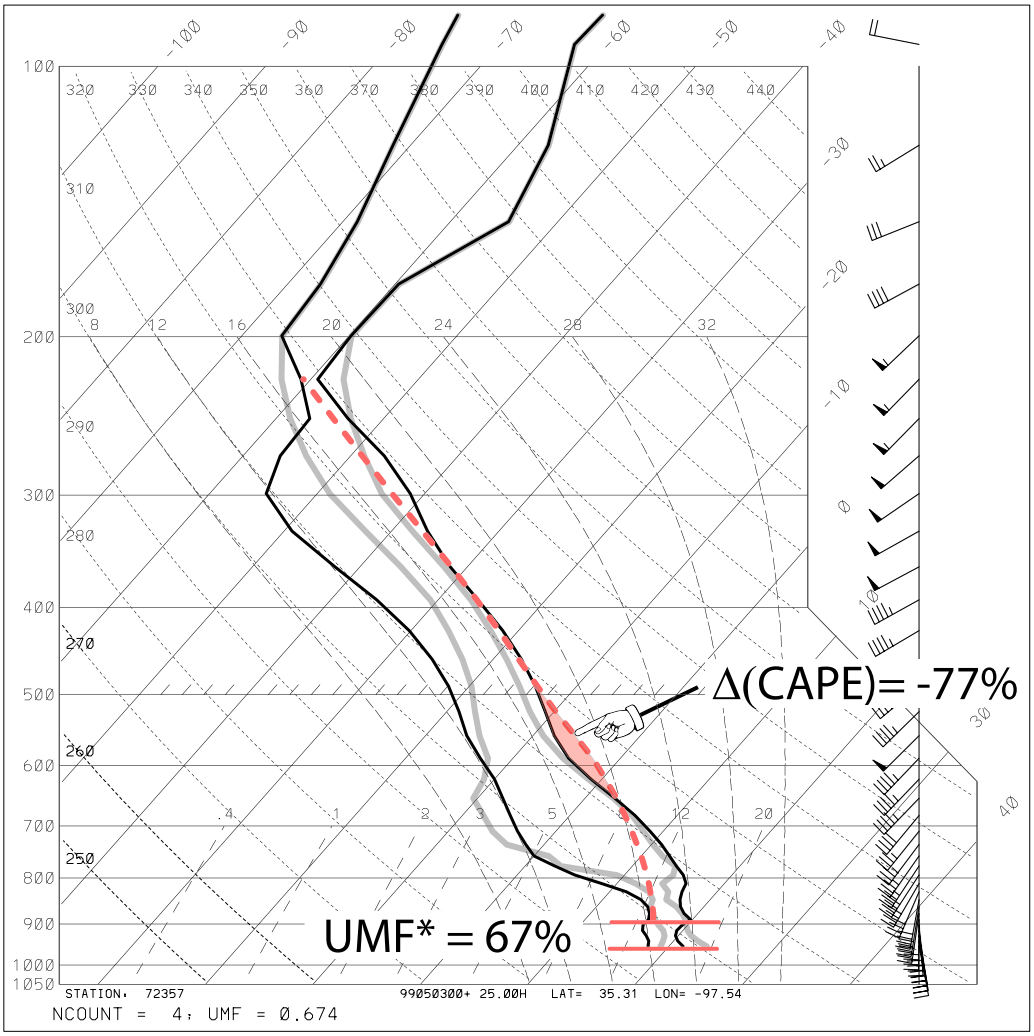

Fig. 4. A depiction of sounding structures and parcel traces from an intermediate stage of the KF computations. Thick, lightly shaded lines show the input sounding. Thick dark lines show an intermediate (modified) sounding generated by the KF scheme. Thick, lightly shaded, dashed line shows the lifted-parcel trace for air originating in the modified USL (top and bottom of USL marked by thick horizontal lines). Shaded area between 500 and 650 hPa indicates positive area (CAPE), while labels indicate that the UMF* = 67% and CAPE has been reduced by 77% at this point in the KF scheme's iterative procedure.

increase to generate the same amount of heating. Even though parameterized downdrafts tend to be the dominant mechanism for stabilization of a sounding by the KF scheme, high lapse rates over a significant portion of the cloud layer can make it very difficult to eliminate up to 90% of the CAPE in a sounding even when downdrafts substantially lower θ_e values in the subcloud layer.

Consider a sounding taken from an intermediate stage of the KF scheme's stabilization procedure (Fig. 4). At this point, the scheme is in the middle of an iterative procedure to determine the final UMF* value. Note that the USL has been cooled and dried considerably by the parameterized downdraft. As a result, a lifted parcel from the modified USL begins the saturated portion of its ascent on a relatively cool moist adiabat. Nonetheless, very little warming has occurred

between about 550 and 700 hPa, where initial lapse rates were nearly dry adiabatic, so the parcel trace still carves out some positive area in this layer. Specifically, the "adjusted" CAPE value has been reduced by only 77% from the original value, so the scheme must increase UMF* beyond 67% to achieve a 90% reduction in CAPE. After two more iterations, the scheme determined that a UMF* value of 100% was necessary to reduce CAPE by 90%.

In this type of environment (*i.e.*, steep low-to-mid level lapse rates) the CAPE reduction per unit mass flux is relatively high for low values of UMF* because parameterized downdrafts introduce sharply lower θ_e air into the USL. As the scheme's iterative procedure moves to higher values of UMF*, however, the θ_e in the USL approaches that of the downdraft and additional mass flux is relatively ineffective at lowering CAPE values. The last vestige of CAPE can be very difficult to eliminate in this type of sounding using the procedures in the KF scheme. In rare cases, UMF* reaches 100% without achieving 90% stabilization. This is the maximum mass flux allowed by the KF scheme.

There is certainly an element of artificiality to this approach, as there is with any convective parameterization. Yet, in a qualitative sense the sensitivity of UMF* to high lapse rates is consistent with modeling studies and observations. For example, Cohen (2000) showed that higher lapse rates in the lower to middle troposphere half are associated with clouds that have relatively large mass flux and penetrate to a greater height. Furthermore, for a given CAPE value, higher lapse rates in the lower part of the cloud layer appear to favor relatively strong parcel accelerations and an enhanced probability of severe thunderstorms, including supercells (Blanchard 1998; Rasmussen and Blanchard 1998).

b. Sensitivity to downdraft θ_e

As suggested above, an important mechanism of stabilization with the KF scheme is replacement of high-θ_e in the USL with low-θ_e air from the parameterized downdraft. Consequently, one would expect that stabilization would be more efficient with lower θ_e values in the downdraft.

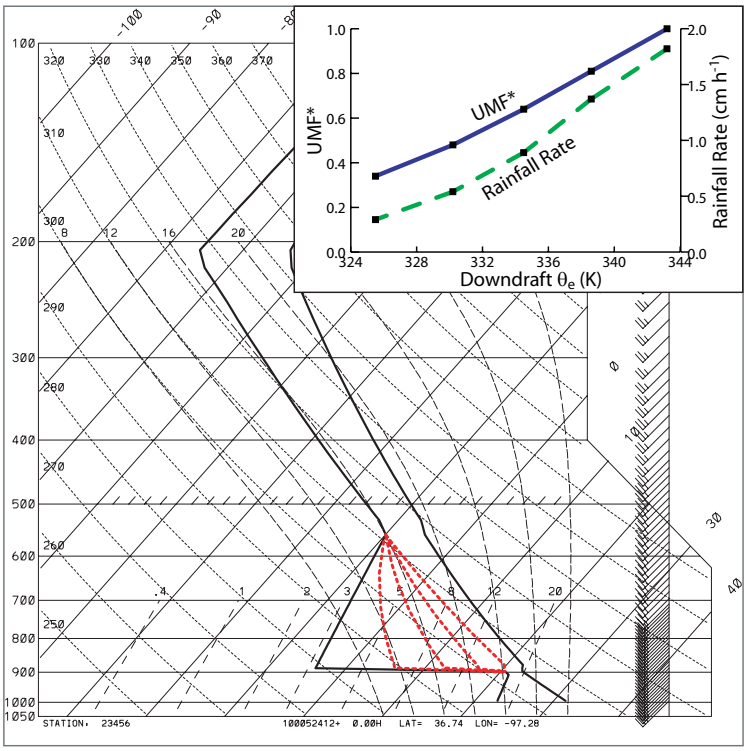

Fig. 5. Idealized sounding modified to evaluate the impact of parameterized downdraft θ_e. Thick dashed lines between about 900 and 550 mb indicate the different dewpoint profiles that were used as input to the KF scheme. Inset shows UMF* and rainfall rate computed by the KF scheme as a function of the different downdraft θ_e values associated with each sounding.

Fig. 5 confirms this sensitivity. In the series of soundings shown here the USL is again the lowest 50 hPa, but the well-mixed layer near the surface is only about 100 hPa deep, so the downdraft (drawing mass from the 150 hPa layer above the USL) is able to tap into the low- θ_e air above the boundary layer. As the mean θ_e of the downdraft source layer is increased from 325K to 343K (by increasing moisture in the elevated mixed layer), UMF* increases from about 0.35 to 1.0. Rainfall rate also increases with this change, reaching almost 2 cm h^{-1} as downdraft stabilizing capacity weakens. It is also worth noting that the CAPE value in each of these soundings is about 4300 J kg^{-1}, so relatively low UMF* values can be diagnosed even with very high CAPE (but low downdraft θ_e) when this instability is efficiently mitigated by parameterized downdraft effects.

4. A realtime convective forecast

The utility of UMF* as a forecasting tool can be demonstrated by examining model predictions of this field for a recent springtime event. At 1200 UTC 9 May 2001, a series of low-amplitude troughs were embedded in fast moving, nearly zonal 500 hPa flow from the Pacific Northwest into the Northern Plains (Fig. 6a). A less energetic pattern prevailed over the rest of the lower forty-eight states, with a broad trough lifting northeastward over the Great Lakes region

and a weak short wave moving eastward across the Southeast. At the surface (Fig. 6b), a ridge of high pressure dominated the Southeast and lower Mississippi river valley, with southerly winds transporting moisture from the Southern Plains toward the upper Mississippi valley. An area of low pressure was moving eastward across the Dakotas, as a trailing cold front moved across parts of Nebraska toward Iowa.

For the purpose of this discussion, we focus on two areas of convective development, one over the Northern Plains and the other over the western Gulf Coast states. In their 0600 UTC Day 1 convective outlook product, SPC forecasters noted that steepening lapse rates and favorable wind fields were expected to create conditions conducive to severe weather development along the cold

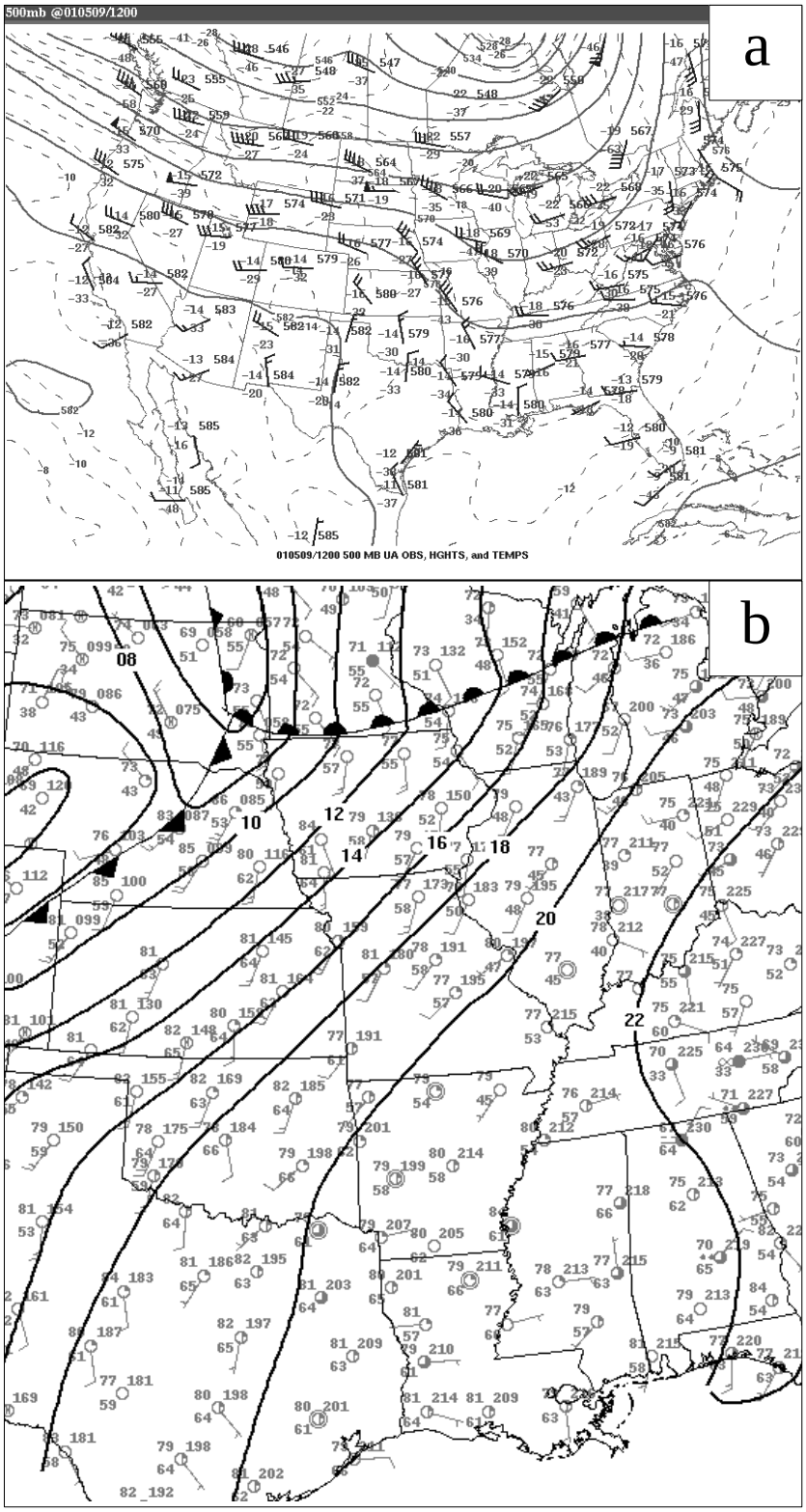

Fig. 6. a) 500 hPa analysis valid 1200 UTC 9 May 2001, with contours of geopotential height (solid lines, 60 m interval) and temperature (dashed lines, 2°C interval) b) Surface analysis valid 1200 UTC 9 May 2001, with frontal analysis and contours of sea-level pressure (solid lines, 2 hPa interval). Station plots are in standard format.

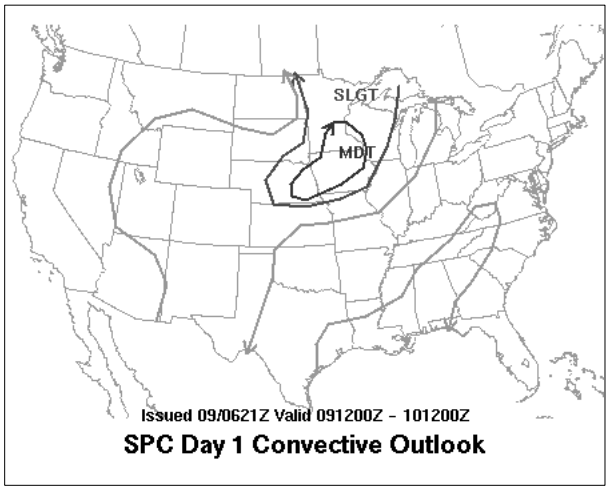

Fig. 7. Storm Prediction Center Day 1 Convective Outlook issued 0621 UTC 9 May 2001. Area enclosed (i.e., to the right of arrows) by outer contours is expected to have greater than 10% coverage of thunderstorms. First interior contour outlines the area of "slight risk" of *severe* thunderstorms, while second interior contour outlines the area of "moderate risk" of *severe* thunderstorms. More information about the SPC Convective Outlook can be found at URL *http://www.spc.noaa.gov/misc/about.html#Levels of risk*

front from southern Minnesota to central Nebraska (Fig. 7). Meanwhile, scattered thunderstorms were expected from eastern Texas eastward into the Appalachians. By 2100 UTC, surface-based CAPE values predicted by the EtaKF were in excess of 4000 J kg^{-1} over eastern Nebraska and more than 3000 J kg^{-1} over a broad surrounding area, while they maximized at 2000 – 2500 J kg^{-1} over Louisiana and eastern Texas (Fig. 8).

Over the Northern Plains, convection developed and rapidly intensified after 2300 UTC along a mesoscale boundary from south-central Minnesota into east-central Nebraska (Fig 9a). The most intense convective activity occurred around 2100 UTC over Louisiana and eastern Texas, where storms were scattered and apparently disorganized on the mesoscale (Fig. 9b). Peak base reflectivity values were somewhat higher over the Northern Plains, though not dramatically different (cf. Figs. 9 a and b). In good agreement with observations, the EtaKF had timely predictions of convective rainfall over both regions (Figs. 9 c and d). 3 h precipitation totals were generally light and similar in magnitude in both areas of concern.

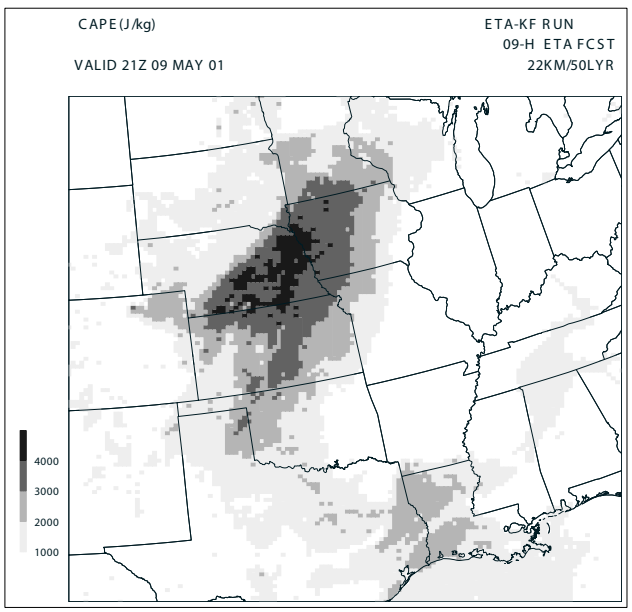

Fig. 8. 9 h forecast of CAPE (J kg^{-1}) from the EtaKF model, valid 2100 UTC 9 May 2001.

Although both the base reflectivity and model-predicted rainfall were similar at these locations, the character of the convection was-

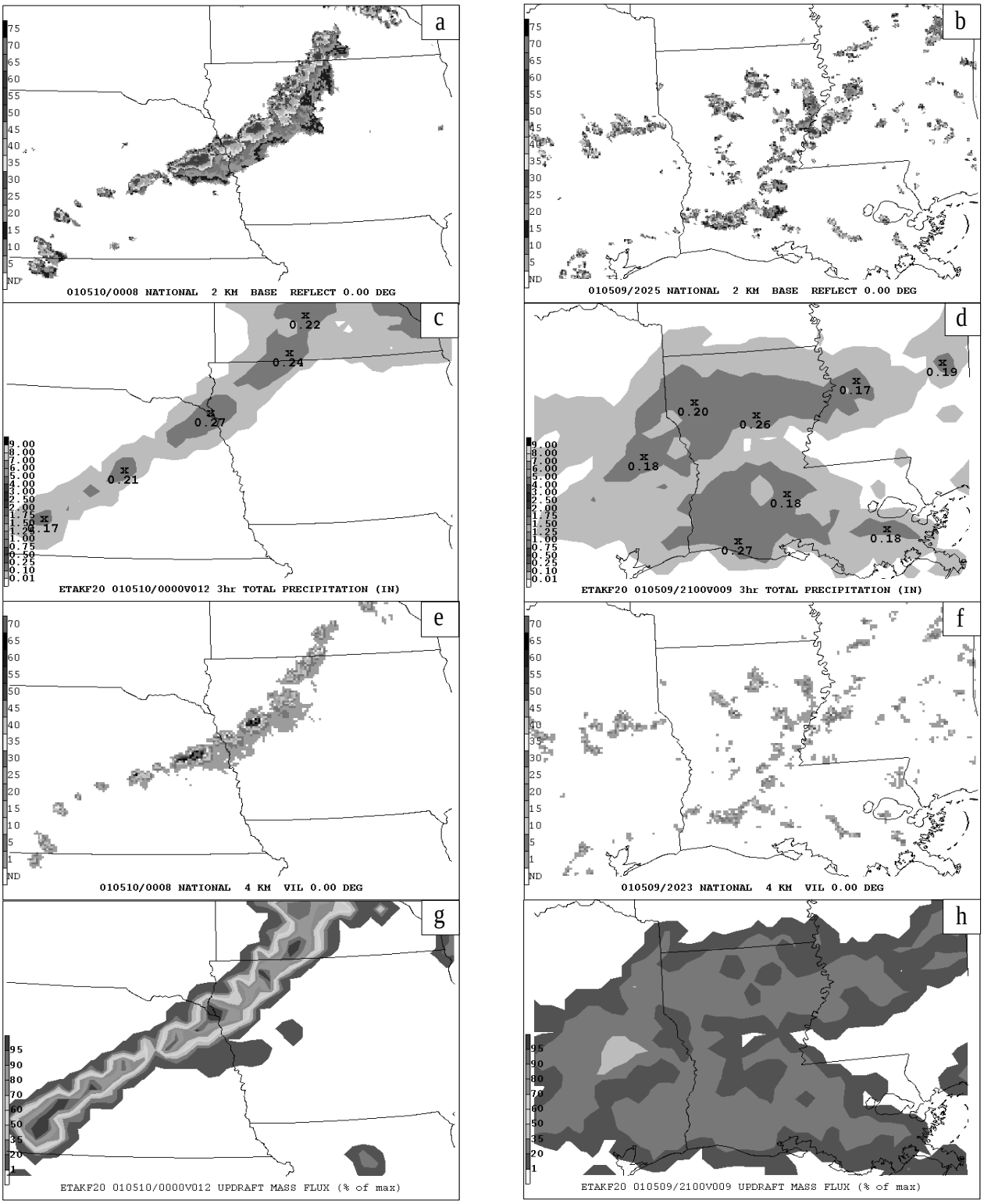

Fig. 9. Comparison of convective characteristics derived from radar (WSR-88D) and EtaKF model forecast for late afternoon/evening 9-10 May 2001. Left-side panels are for the Iowa/Nebraska region while right-side panels are for Louisiana and surrounding areas. a) and b) showbase reflectivity (dBz, 0.5^{o} elevation) valid 10/0008 UTC and 09/2025 UTC, respectively; c) and d) show 3 h accumulated precipitation ending 10/0000 UTC and 09/2100 UTC, respectively; e) and f) show vertically integrated liquid (kg m^{-2}) valid 10/0008 UTC and 09/2023 UTC, respectively; g) and h) show UMF* (%, maximum over previous hour) valid 10/0000 UTC and 09/2100 UTC, respectively.

very different. In the Northern Plains, thunderstorms were severe, with many reports of large hail,

damaging winds, and several tornadoes (National Climatic Data Center 2001). Meanwhile, storms were distinctly non-severe over the Gulf Coast states, with a single large-hail report coming in from this region. This difference in character was better reflected by a radar-derived VIL (Vertically Integrated Liquid) plots, showing numerous pixels with up to of 70 kg m^{-2} over northern Iowa, but isolated maxima of only 50 kg m^{-2} over Louisiana (Figs. 9 e and f). Most significantly, a stark contrast was provided by the EtaKF's UMF* field. UMF* values approached 100% along the convective line in the Northern Plains, but well below 50% over most of Louisiana and eastern Texas (Figs. 9 g and h). This disparity in UMF* provided forecasters with a clear indication of the different character of convective activity that was possible in these two separate regions.

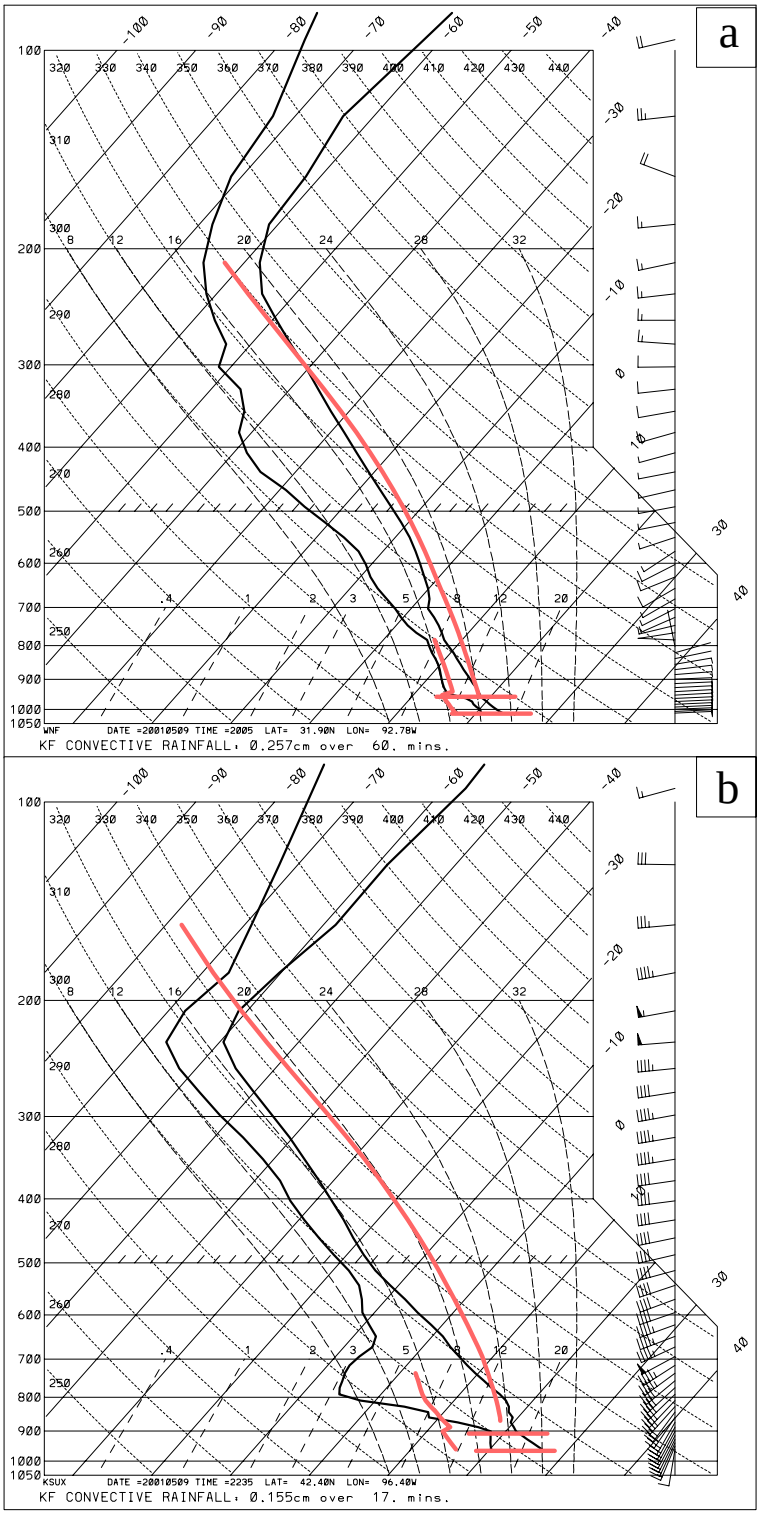

Fig. 10. EtaKF model forecast soundings from the convective environments shown in Fig. 8, with the input sounding and updraft and downdraft traces predicted predicted by the KF scheme as in Fig 1a. a) from grid point near Winnfield, LA, valid at 2005 UTC 9 May 2001. b) from near Sioux City, IA, valid 2235 UTC 9 May 2001.

As stressed above, UMF* values are closely related to sounding structure. A (pre-convective) model forecast sounding taken from west-

central Louisiana is representative of the surrounding environment along the Gulf Coast. This sounding shows a very moist boundary layer with little convective inhibition and moderate instability (Fig. 10a). The updraft predicted by the KF scheme is marginally buoyant throughout the depth of the cloud, but note that the parcel trace shown in Fig. 10a includes the effects of entrainment, giving the misleading impression that CAPE (which is typically computed assuming undiluted ascent) is quite small. In contrast, a (pre-convective) model sounding from northwest Iowa shows a moderately moist boundary layer, a moderately strong inhibition layer, and extreme instability aloft (Fig. 10b). Environmental lapse rates are nearly dry-adiabatic from 800 hPa up to 500 hPa, which would support rapid acceleration of buoyant parcels originating in the boundary layer. Note that the KF updraft deviates sharply from moist adiabatic ascent due to entrainment, but even this diluted updraft is strongly buoyant through the depth of the cloud.

5. Concluding comments

Operational NWP models do not provide explicit forecasts of the vigor of deep convection. They *do* provide predictions of convective rainfall rate, but forecaster experience suggests that this field is not a reliable indicator of convective intensity. When we first started running the KF parameterization in the Eta model several years ago (Kain et al. 1998), this contradiction became apparent. In examining several numerical forecasts of severe weather events, we noted that convective rainfall coverage was often correctly predicted by the model when severe weather occurred, but light rainfall amounts generated by the scheme failed to indicate the severity of the convection. Similar behavior occurred with other convective parameterizations that we evaluated.

Further examination of the EtaKF forecasts in these cases revealed that even though rainfall rates were low, the KF scheme was feeding back very strong temperature and moisture tendencies to resolved scales in the model. We sought to convey this information to users by supplementing convective rainfall output with some measure of the strength of parameterized adjustments to the

model's atmosphere. We settled on UMF* because it can be readily conceptualized as the amount of mass flowing through cloud base and it can be simply expressed on a scale from 0 to 1.

Output from our twice-daily runs of the EtaKF is supplied directly to the SPC on N-AWIPS workstations, and forecaster feedback on the UMF* field has been very positive. Since UMF* is a unique predictor of convective intensity and because operational experience suggests it has value, examination of this field has become a routine part of the forecast preparation process at the SPC. In addition, forecasters at some other National Weather Service offices have begun to use this product as they have recognized its utility (M. Foster[1], personal communication). External users can access output from the EtaKF runs at URL http://www.nssl.noaa.gov/etakf.

In this paper, an overview of the KF scheme has been presented and the relationship between updraft mass flux and other elements of the scheme has been described. The magnitude of UMF* generated by the scheme is a function of the procedures and closure assumptions of the KF scheme. More importantly, it is a function of the sounding structure, with the highest values of UMF* typically associated with high lapse rates in the lower half of the convective cloud layer. Given this association, UMF* may be a valuable indicator of the potential for severe weather, since the *conditional* probability of severe convection (*i.e.*, the probability that convection will be severe if any thunderstorms develop) appears to increase as lapse rates in the lower to middle troposphere increase (Blanchard 1998; Cohen 2000).

Operational experience suggests that UMF* correlates well with observed measures of convective intensity, such as lightning flash density, severe weather reports, and radar-derived Vertically-Integrated Liquid water (VIL). An independent study by Allen and Pickering (2002) suggests that parameterized updraft mass flux is a good predictor of lightning flash density in a climatological sense (*i.e.*, not necessarily on precise time and space scales). We are currently

1. Mike Foster is the Meteorologist In Charge at the Norman, OK National Weather Service Forecasting Office.

developing objective procedures to correlate UMF* with different observed measures of convective intensity on mesoscale grids, following the techniques described by Baldwin et al. (2001).

We encourage severe weather forecasters to examine the UMF* field when it is available. Moreover, we urge developers of other mass flux parameterizations of convection to investigate the utility of this field in the context of their scheme. Finally, we encourage model developers to explore the possibility of extracting other potentially useful "internal" forecast fields from NWP models.

Acknowledgements

Internal reviews of this manuscript by Matt Wandishin and Dave Stensrud of NSSL were very helpful.

REFERENCES

Allen, D. and K. Pickering, 2002: Evaluation of lightning flash rate parameterizations for use in a global chemical-transport model. Submitted to *J. Geophys. Res.*

Baldwin, M. E., S. Lakshmivarahan, and J. S. Kain, 2001: Verification of mesoscale features in NWP models. *Preprints, Ninth Conference on Mesoscale Processes*, Amer. Meteor. Soc., Ft. Lauderdale, FL, July 30 – August 2, 2001.

Black, T.L., 1994: The new NMC mesoscale Eta model: Description and forecast examples. *Wea. Forecasting* **9**, 265-278.

Blanchard, D. O., 1998: Assessing the vertical distribution of convective available convective energy. *Wea. Forecasting*, **13**, 870-877.

Bluestein, H. B., and C. R. Parks, 1983: A Synoptic and Photographic Climatology of Low-Precipitation Severe Thunderstorms in the Southern Plains. *Mon. Wea. Rev.*, **111**, 2034–2046.

Benjamin, S. G., J. M. Brown, K. J. Brundage, B. E. Schwartz, T. G. Smirnova, and T. L. Smith, 1998: The operational RUC-2. *Preprints, 16th conf. on Weather analysis and Forecasting*, Phoenix, AZ, Amer. Meteor. Soc., 249-252.

Cohen, C., 2000: A quantitative investigation of entrainment and detrainment in numerically simulated cumulonimbus clouds. *J. Atmos. Sci.*, **57**, 1657-1674.

Ferrier, B. S., J. Simpson, and W.-K. Tao, 1996: Factors responsible for precipitation efficiencies in midlatitude and tropical squall simulations. *Mon. Wea. Rev.*, **124**, 2100-2125.

Fritsch, J. M., C. F. Chappell and L. R. Hoxit, 1976: The use of large-scale budgets for convective parameterization. *Mon. Wea. Rev.*, **104**, 1408-1418.

Janji_, Z. I., 1994: The step-mountain eta coordinate model: Further developments of the convection, viscous sublayer, and turbulence closure schemes. *Mon. Wea. Rev.*, **122**, 927-945.

Johns, R. H., and C. A. Doswell III, 1992: Severe Local Storms Forecasting. *Wea. Forecasting*, **7**, 588–612.

Kain, J.S., and J.M. Fritsch, 1990: A one-dimensional entraining/detraining plume model and its application in convective parameterization. *J. Atmos. Sci.*, **47**, 2784-2802.

Kain, J.S., and J.M. Fritsch, 1992: The role of the convective "trigger function" in numerical forecasts of mesoscale convective systems. *Meteor. Atmos. Phys.*, **49**, 93-106.

Kain, J.S., and J.M. Fritsch, 1993: Convective parameterization for mesoscale models: The Kain-Fritsch scheme. *The representation of cumulus convection in numerical models.* Meteor. Monogr., No. 24, Amer. Meteor. Soc., 165-170.

Kain, J. S., M. E. Baldwin, D. J. Stensrud, T. L. Black, and G. S. Manikin, 1998: Considerations for the implementation of a convective parameterization scheme in an operational mesoscale model. *Preprints, 12th Conference on Numerical Weather Prediction*, Phoenix, AZ, Amer. Meteor. Soc., 103-106.

Knupp, K. R., 1989: Numerical simulation of low-level downdraft initiation within precipitating cumulonimbi: Some preliminary results. *Mon. Wea. Rev.*, **117**, 1517-1529.

Knupp, K. R., and W. R. Cotton, 1985: Convective cloud downdraft structure: An interpretive survey. *Reviews of Geophysics*, **23**, 183-215.

National Climatic Data Center, 2001: Storm Data. Vol. 43, No. 5, 306 pp. [Available from the National Climatic Data Center, Asheville, NC 28801]

Rasmussen, E. N., and D. O. Blanchard, 1998: A baseline climatology of sounding-derived supercell and tornado forecast parameters. *Wea. Forecasting* **13**, 1148-1164.

Srivastava, R. C., 1985: A model of intense downdrafts driven by the melting and evaporation of precipitation. *J. Atmos. Sci.*, **44**, 1752-1773.

Wakimoto, R. M., 1985: Forecasting Dry Microburst Activity over the High Plains. *Mon. Wea. Rev.*, **113**, 1131–1143.

Weisman, M. L., and J. B. Klemp, 1982: The dependence of numerically simulated convective storms on vertical wind shear and buoyancy, *Mon. Wea. Rev.*, **110**, 504-520.

Figure Captions

Fig. 1. An idealized sounding (thick dark curves) with a) the updraft and downdraft traces and b) the modified sounding resulting from mass rearrangements, both predicted by the KF scheme (thick lighter curves). The thick lighter horizontal lines near the surface denote the top and bottom of the updraft source layer (USL).

Fig. 2. Idealized sounding (solid curves) modified to evaluate the impact of increasing lapse rates in the 750-500 mb layer. Dashed lines show modified temperature profiles with higher lapse rates and CAPE values. Inset shows UMF* and rainfall rate predicted by the KF scheme as a function of the different (undilute parcel) CAPE values corresponding to the different temperature profiles.

Fig. 3. Idealized sounding modified to evaluate the impact of moistening in the USL (top and bottom denoted by light thick horizontal lines near the surface). Thick dashed lines between 1000 and 950 mb indicate USL dewpoint profiles in different modified soundings while thick dashed lines aloft denote the undilute parcel trace corresponding to the modified USL dewpoints. Note that the input sounding is <u>not</u> modified above the top of the USL. Inset shows UMF* and rainfall rate computed by the KF scheme as a function of the different CAPE values associated with each dewpoint profile.

Fig. 4. A depiction of sounding structures and parcel traces from an intermediate stage of the KF computations. Thick, lightly shaded lines show the input sounding. Thick dark lines show an intermediate (modified) sounding generated by the KF scheme. Thick, lightly shaded, dashed line shows the lifted-parcel trace for air originating in the modified USL (top and bottom of USL marked by thick horizontal lines). Shaded area between 500 and 650 hPa indicates positive area (CAPE), while labels indicate that the UMF* = 67% and CAPE has been reduced by 77% at this point in the KF scheme's iterative procedure.

Fig. 5. Idealized sounding modified to evaluate the impact of parameterized downdraft θ_e. Thick dashed lines between about 900 and 550 mb indicate the different dewpoint profiles that were used as input to the KF scheme. Inset shows UMF* and rainfall rate computed by the KF

scheme as a function of the different downdraft θ_e values associated with each dewpoint profile.

Fig. 6. a) 500 hPa analysis valid 1200 UTC 9 May 2001, with contours of geopotential height (solid lines, 60 m interval) and temperature (dashed lines, 2^{o}C interval) b) Surface analysis valid 1200 UTC 9 May 2001, with frontal analysis and contours of sea-level pressure (solid lines, 2 hPa interval). Station plots are in standard format.

Fig. 7. Storm Prediction Center Day 1 Convective Outlook issued 0621 UTC 9 May 2001. Area enclosed (i.e., to the right of arrows) by outer contours is expected to have greater than 10% coverage of thunderstorms. First interior contour outlines the area of "slight risk" of *severe* thunderstorms, while second interior contour outlines the area of "moderate risk" of *severe* thunderstorms. More information about the SPC Convective Outlook can be found at URL *http://www.spc.noaa.gov/misc/about.html#Levels of risk*

Fig. 8. 9 h forecast of CAPE (J kg^{-1}) from the EtaKF model, valid 2100 UTC 9 May 2001.

Fig. 9. Comparison of convective characteristics derived from radar (WSR-88D) and EtaKF model forecast for late afternoon/evening 9-10 May 2001. Left-side panels are for the Iowa/ Nebraska region while right-side panels are for Louisiana and surrounding areas. a) and b) showbase reflectivity (dBz, 0.5^{o} elevation) valid 10/0008 UTC and 09/2025 UTC, respectively; c) and d) show 3 h accumulated precipitation ending 10/0000 UTC and 09/2100 UTC, respectively; e) and f) show vertically integrated liquid (kg m^{-2}) valid 10/ 0008 UTC and 09/ 2023 UTC, respectively; g) and h) show UMF* (%, maximum over previous hour) valid 10/ 0000 UTC and 09/2100 UTC, respectively.

Fig. 10. EtaKF model forecast soundings from the convective environments shown in Fig. 8, with the input sounding and updraft and downdraft traces predicted predicted by the KF scheme as in Fig 1a. a) from grid point near Winnfield, LA, valid at 2005 UTC 9 May 2001. b) from near Sioux City, IA, valid 2235 UTC 9 May 2001.